NUMERICAL MODELING OF PEAT BURNING PROCESSES IN A VORTEX FURNACE WITH COUNTERCURRENT SWIRL FLOWS

by

Andriy REDKO[a*], Burda YURII[a], Rafael DZHYOIEV[b], Igor REDKO[c], Volodymyr NORCHAK[a], Serhii PAVLOVSKIIY[a], and Oleksandr REDKO[a]

[a]Department of Heat, Gas Supply, Ventilation and Using Thermal Second Energy Resources, Kharkov National University of Civil Engineering and Architecture, Kharkov, Ukraine
[b]Public Corporation "City Gas Supply of Kharkov", Kharkov, Ukraine
[c]Department of Heat Engineering, Kiev National University of Civil Engineering and Architecture, Kiev, Ukraine

Original scientific paper
https://doi.org/10.2298/TSCI190305158R

The paper presents the process of peat burning in a swirl furnace with countercurrent swirl flows and the results of a numerical study. The cyclone-vortex technology of solid fuel combustion allows the furnace volume of a boiler unit, its dimensions and weight to be reduced. The aim of the work is a numerical study of the combustion of pulverized peat in a cylindrical vortex furnace with countercurrent swirl flows. The results of computer simulation of the combustion of pulverized peat with a moisture content of 40%, an ash content of 6%, and a higher heat of combustion Q_H^p = 12.3 MJ/kg are presented. The results of the influence of the design parameters of the furnace and heat load (from 100-15%) are given as well. When the heat load is reduced to 15%, the entrainment of unburnt particles increases. The cooled and adiabatic furnace is studied. A significant entrainment of unburned particles is observed in a cooled furnace. The fields of temperature distribution, gas velocity, and particle trajectory in the volume and at the outlet of the furnace are determined. The 3-D temperature distribution in the furnace volume indicates the combustion of peat particles at temperatures (1300-1450 °C). Values of the tangential velocity of a swirl flow near the furnace outlet reach 150-370 m/s, which ensures the efficiency of separation of fuel particles and a reduction in heat loss due to mechanical underburning (up to 0.06%). The results of a numerical study show that the diameter of peat particles affects the combustion process, namely coke of particles with an initial diameter from 25-250 μm burns out by 96%, and particles with a diameter of about 1000 μm are carried away from the furnace and do not burn. The furnace provides a complete combustion of dust particles of peat by 99.8% and volatiles by 100%.

Key words: *combustion processes, numerical modeling, peat, vortex furnace, countercurrent swirl flows*

* Corresponding author e-mal: andriy.ua-mail@ukr.net

Introduction

Peat is a renewable fossil fuel. Peat deposits in Western Europe are 51 million hectares, in Asia – over 100 million hectares, in North America – over 18 million hectares. The largest deposits of peat (billion tons) are in Canada – 170, Russia – 162, Indonesia – 78.5, and USA – 36.3. In Ukraine 3118 peat deposits with geological reserves of about 2.2 billion tons have been explored. The total area of deposits is about 3 million hectares, the balance reserves of peat are about 735 million tons.

Modern technologies for the thermochemical conversion of peat are gasification and pyrolysis.

The main disadvantage of gasification is the low calorific value of the produced gas (Q_H^p = 1400 kcal/m^3) and the combustion temperature (about 1500 °C). Pyrolysis allows gaseous, liquid and solid products to be obtained [1].

In the process of thermochemical processing of peat, many chemical reactions (homogeneous and heterogeneous) occur that determine the possibility of processing peat. New peat gasification methods are currently being developed the energy of gaseous fuel during pyrolysis being not more than 20% of the initial energy of peat.

Peat fuel production is in its infancy. Biofuel is not hygroscopic, has a high volumetric calorific value which allows providing its transportation and storage. The total yield of gaseous products is 0.34 m^3 per kg of initial dry product the calorific value being Q_H^p = 11.7 MJ/kg (up to 15 MJ/kg). Therefore, the direction of burning peat in heating boilers of small and medium power is being developed.

Increasing the efficiency of energy saving in heat supply systems is possible using the low-grade solid-fuels, wood and coal waste [2, 3]. However, the grate furnaces of boilers need modernizing for burning low-calorific solid fuels with high humidity and ash content and polydisperse components [4]. The fluidized bed furnaces need to improve the particle separation, that are carried out, and their return to the furnaces to finish the combustion [5]. Vortex furnaces are effective, but they are characterized with significant combustible losses which require their modernization as well [6]. The main advantages of low temperature vortex combustion technology include improved environmental indicators, stability of solid fuel ignition and burning without inflammation by gas or fuel oil, usage of non-mill schemes of fuel preparation. Low temperature vortex technology of solid-fuel combustion can be realized in a traditional chamber furnace by modernizing it. The low temperature vortex technology provides combustion of such solid fuels as: coal and brown coal, oil shales, peat, timber process waste, and other types of biofuel.

Low temperature vortex technologies implemented in chamber furnaces use the principle of low temperature solid-fuel combustion within the conditions of multiple circulation of particles in a chamber furnace. In chamber furnaces, two combustion zones are performed: vortex and direct-flow. In the furnace the active combustion zone occupies a significant volume of the combustion space which allows reducing the maximum temperature in the vortex furnace by 100-300 °C. Nevertheless, the volume of the furnace is high, that determines the size and the metal intensity of the boiler. In the chamber furnace which realizes a disconnected vortex diagram of the furnace process, large swirls do not ensure the consistency of the flow. The cyclonic-vortex technology of solid-fuel combustion allows reducing the furnace volume of the boiler, its size and mass. Intensive mixing of fuel and air particles in a swirl flow ensures intensive heat and mass exchange and fuel combustion. For boilers with a thermal capacity of less than 30 MW, it is difficult to organize low temperature vortex tech-

nology. Therefore, the combustion of local fuel waste and biofuels in boilers of low power (up to 3 MW) is of particular interest. The usage of the cyclonic-vortex technology as an extension furnace of a boiler for the combustion of liquid and gaseous fuels makes it possible to place extension furnaces in the furnace cavity [6]. This technology for solid-fuel combustion has not been studied enough.

In the process of the energy usage of fuels ash properties determine the technology and combustion regime. The method of slag removal is determined by the temperature of the normal liquid slag removal, t_r, of gases in the lower part of the furnace. Temperature, t_r, depends on the iron content in the slag and the degree of its oxidation as well as the calcium oxide content. Slag composition of peat is SiO^2 (25-40%), Al_2O_3 (5-30%), CaO (30-55%), MgO (0-10%), Fe_2O_3 (5-30%), FeO (0-30%) with the ratio $SiO_2/Al_2O_3 = 1.33>1.2$ being fulfilled. For furnaces with liquid ash removal the ratio SiO_2/Al_2O_3 should be more than 1.2 [7]. For peat ash the melting point is 1070-1200 °C. In single-shaft furnaces to obtain liquid slag and remove it from the furnace, the bottom part of the furnace is made with a knuckle, sorting a small volume for the combustion chamber and slag smelting chamber. Improving the fractional composition of fuel particles by reducing the content of coarse fractions provides more complete fuel combustion and the reduction of mechanical underburning losses, q_4.

In the vortex furnace with swirl flows and one-way hinge there is the forced combustion chamber for slag melting [8]. In the furnace the slag is up to 60%. The thermal stress is 580-700 kW/m^3 in the combustion chamber and slag smelting chamber. The furnace is less sensitive to the quality of the combustion when it is operated in variable conditions and under reduced load. Further increase of the intensity of the combustion process in the liquid ash-removal furnaces in a wide range of thermal charge is in double-chamber furnaces [8], cyclonic furnaces [9] and in furnaces with vertical extension furnaces [10]. The loss of heat from the chemical incompleteness of combustion, q_3, in the brown coal cyclone is $q_3 = 0.5\%$ and the heat loss from combustible losses is $q_4 = 0.2\%$. Thermal stress of the cyclone in extention furnaces) is 1300 kW/m^3, in furnaces with vertical extension it is 760-870 kW/m^3 and in double-chamber furnaces, 700-810 kW/m^3. In cyclone furnaces ash in liquid form is up to 85-90%. Horizontal cyclones are not recommended for solid fuel combustion because of its insufficiently stable, intensive and economical combustion.

Furnaces with vertical extention ensure combustion of coarse milling brown coal dust with fractions up to 1000 microns. The thermal stress of the volume of the vertical cyclone is 1.1-1.4 MW/m^3, the total thermal losses are $q_3 + q_4 = 0.5\%$, the temperature of gases is 1550-1600 °C. For boilers of thermal capacity from 4 to 30 MW the usage of high temperature fluidized bed technology is effective. However, high rates of gas flow require significant size of the combustion volume, and multiple circulation of solid particles requires highly efficient separation devices.

Vortex technology of solid fuel combustion in cyclone furnaces of pulverized-coal boilers and the organization of tangential combustion in an upward vortex are studied in [11-13].

Using numerical methods, the basic characteristics of the BKZ-75 boiler with forced partial stop of the coal dust supply through the burners are studied [14-16].

Numerical researches to study the influence of air-flow temperature and a fossil fuel particle rate on sufficient conditions of ignition in a *coal dust-air* system are given [17].

The axisymmetric problem of heat and mass transfer processes in a *coal particle-air* system was solved in a spherical co-ordinate. Mathematical model includes the system of non-linear non-stationary differential equations in dimensionless variables and corresponding initial and boundary conditions.

The burning of lignite in atmospheric air enriched with oxygen is studied [18].

In this work, the oxygen-enriched combustion behaviour of indigenous lignite was measured by a thermogravimetric analyser. Combustion tests were carried out in N_2/O_2 atmosphere with an oxygen content ranging from 21 to 70 vol.%. The results indicated that the relationship between calorific value per unit time and oxygen concentration fit the exponential function exactly

A new processing scheme of plant raw materials is presented in [19], which includes mechanical and chemical treatment of the plant raw materials and dividing the powder product into particles and non-lignified tissues being rich in lignine and cellulose, respectively.

Technological and thermal schemes of biofuel combustion plants are studied in [20].

Theoretical background

Numerical studies of solid fuel combustion processes are performed in the works [11-19, 21-25]. While making the mathematical description of physical and chemical processes in the furnace, the following basic assumptions are made in this work, namely the flow of the carrier gas medium is 3-D, chemically reacting, quasistationary, incompressible, turbulent, multicomponent; the rate of gas-phase chemical reactions is infinitely high; the gas mixture is in a state of thermodynamic equilibrium; buoyancy, bulk viscosity and viscous heating are neglected; peat particles are spherical, polydisperse; the volume occupied by the particles is neglected; burning of peat particles includes the processes of evaporation and combustion of volatiles and the burning of the coke residue; heat exchange by radiation is taken into account; turbulence is isotropic; particles do not affect turbulence parameters; turbulent dispersion of particles is taken into account. A dust-peat air mixture is modeled as a two-phase mixture with the Euler description of the gas phase (a continuous medium) and the Lagrangian description of the movement of peat particles (a trajectory model). The phase interaction is taken into account on the basis of the *particle-source in the cell* model [26], according to which the presence of a particle in the flow manifests itself through additional sources in the equations of conservation of the continuous phase. The instantaneous thermochemical state of the flow is considered to be uniquely determined by the conservative scalar quantity, *i.e.* the dimensionless Schwab-Zeldovich function, which has the meaning of the mass fraction of reduced fuel. The interaction of chemical processes and turbulence is described statistically using the probability distribution density function. Under the above assumptions, the behaviour of the gas phase is described by a system of partial differential equations consisting of Reynolds-averaged Navier-Stokes equations, two equations of the k-ε type turbulence differential model [27], conservation equations for the dimensionless Schwab-Zeldovich functions, f_n, and for pulsations of these functions $g_n = f_n^{'2}$ [28] and the integro-differential equation of radiation transfer [29-31]:

$$\rho \frac{\partial u_j}{\partial x_j} = S_n \tag{1}$$

$$\rho \frac{\partial u_j u_i}{\partial x_j} - \frac{\partial p}{\partial x_i} - \frac{\partial \tau_{ij}}{\partial x_j} = S_{fi}, \quad j = 1,2,3 \tag{2}$$

$$\rho \frac{\partial u_j h}{\partial x_j} - \frac{\partial}{\partial x_j}\left(\frac{\mu}{\mathrm{Pr}} + \frac{\mu_m}{\mathrm{Pr}_m}\right)\frac{\partial h}{\partial x_j} = S_q, \quad j = 1,2,3 \tag{3}$$

$$\rho \frac{\partial u_j k}{\partial x_j} - \frac{\partial}{\partial x_j}\left(\mu + \frac{\mu_m}{\sigma_k}\right)\frac{\partial k}{\partial x_j} - \rho\left(G - \varepsilon\right) = 0, \quad j = 1,2,3 \tag{4}$$

$$\rho\frac{\partial u_j\varepsilon}{\partial x_j}-\frac{\partial}{\partial x_i}\left(\mu+\frac{\mu_m}{\sigma_\varepsilon}\right)\frac{\partial\varepsilon}{\partial x_j}-\rho\left(G_{\varepsilon 1}G-G_{\varepsilon 2}\varepsilon\right)=\frac{\varepsilon}{k}=0,\quad j=1,2,3 \tag{5}$$

$$\rho\frac{\partial\left(\vec{\mathrm{u}}f_n\right)}{\partial x_j}=\frac{\partial}{\partial x_j}\left(\frac{\mu_m}{\sigma_m}\frac{\partial f_n}{\partial x_j}\right)+S_n,\quad j=1,2,3;n=1,2,3 \tag{6}$$

$$\rho\frac{\partial\vec{\mathrm{u}}g_n}{\partial x_j}=\frac{\partial}{\partial x_j}\left(\frac{\mu_m}{\sigma_m}\frac{\partial g_n}{\partial x_j}\right)+C_g\mu_m\left(\frac{\partial f_n}{\partial x_i}\right)^2-C_d\rho\frac{\varepsilon}{k}g_n,\quad j=1,2,3;n=1,2,3 \tag{7}$$

$$\frac{1}{\beta_0}\frac{\mathrm{d}I\left(\vec{\mathrm{r}},\vec{\mathrm{s}}\right)}{\mathrm{d}s}+I\left(\vec{\mathrm{r}},\vec{\mathrm{s}}\right)=\left(1-\omega_0\right)I_b\left(\vec{\mathrm{r}}\right)+\frac{\omega_0}{4\pi}\int_{\Omega'=4\pi}I\left(\vec{\mathrm{r}},\vec{\mathrm{s}}\right)\mathrm{d}\Omega' \tag{8}$$

$$\tau_{ij}=\left(\mu+\mu_m\right)\left(\frac{\partial u_i}{\partial x_j}+\frac{\partial u_j}{\partial x_i}\right) \tag{9}$$

Turbulent viscosity is determined by the Kolmogorov-Prandtl formula [32].

$$\mu_m=C_\mu\rho\frac{k^2}{\varepsilon} \tag{10}$$

$$k=\frac{1}{2}u_i'u_i' \tag{11}$$

$$\varepsilon=\frac{1}{2}\nu\left(\frac{\partial u_j'}{\partial x_i}+\frac{\partial u_i'}{\partial x_j}\right)^2 \tag{12}$$

$$h=\sum_i Y_i\left(\Delta h_{fi}^0+\int_{T^0}^{T}c_{pi}\left(T\right)\mathrm{d}T\right) \tag{13}$$

The generation of kinematic energy of turbulence due to shear stresses is determined by the formula:

$$G=\mu_m\frac{\partial u_i}{\partial x_j}\left(\frac{\partial u_i}{\partial x_j}+\frac{\partial u_j}{\partial x_i}\right) \tag{14}$$

Equation (8) is written on the basis of the assumption of quasistationary, coherent and isotropic radiation transfer [33]. The dimensionless Schwab-Zeldovich function is determined by the expression:

$$f_n=\frac{Z_q-Z_{q.O}}{Z_{q.F_1}-Z_{q.O}} \tag{15}$$

$$f_1+f_2+f_0=1 \tag{16}$$

where Z_q is the mass fraction of the element q, the indices F_1 and O refer to the primary fuel and oxidizing agent, respectively. All thermochemical scalars φ_i (mass fractions of chemical components, density and temperature) depend exclusively on f_n:

$$\varphi_i=\int_{00}^{11}\varphi_i\left(f_1,f_2,h\right)P_2\left(f_2\right)\mathrm{d}f_1\mathrm{d}f_2 \tag{17}$$

The system of eqs. (1)-(7) is not closed. The connection between the variables p, T, and ρ necessary for its closure is established by the equation of state of a mixture of ideal gases:

$$p = \mathrm{R}\rho T \sum_i \frac{Y_i}{M_i} \tag{18}$$

To determine the source terms (mass, heat, momentum) S_n in eqs. (1) and (6), S_{fi} in eq. (2), and S_q in eq. (3), the model of interphase interaction is used, which is implemented by alternately solving the dispersed and continuous phase equations until solutions to both phases are established. The whole range of initial peat particle sizes is divided into a finite number of discrete intervals; each represents an average diameter for which the trajectory and heat-and mass exchange are calculated. Moreover, each simulated particle is a *package* of particles with the same trajectories. The particle size distribution is described by the Rosin-Rammler formula:

$$Y_d = \mathrm{e}^{-\left(d/\bar{d}\right)^n} \tag{19}$$

Particle trajectories are modeled by integrating the equation of balance of forces acting on the particle, balancing the inertia of the particle with the force of aerodynamic drag:

$$\frac{\mathrm{d}u_{pj}}{\mathrm{d}t} = -\frac{3\rho C_R}{4\rho_p d_p}\left(u_{pj} - u_j\right)\sqrt{\sum_j \left(u_{pj} - u_j\right)^2}, \quad j = 1,2,3 \tag{20}$$

To calculate C_R, the empirical function C_R (Re_p) for a single sphere is used. The heat and mass exchange of peat particles is described by three models: the heat exchange model of an inert particle; a volatile yield model and a coke residue burnout model.

The model of heat exchange of an inert particle is applied until the particle temperature T_p does not exceed the volatile yield temperature T_v. In this case, the particle temperature is assumed to be constant in volume and varies in accordance with the heat balance determined:

$$m_p c_p \frac{\mathrm{d}T_p}{\mathrm{d}t} = \alpha S_p \left(T_\infty - T_p\right) \tag{21}$$

The volatile yield model is used when the temperature of the peat particle reaches the temperature of the volatile yield onset T_v and remains valid until the particle mass m_p exceeds the initial mass of non-volatile components in the particle: $T_p \geq T_v$; $m_p \geq (1 - f_{v,0}).m_{p,0}$

The heat and mass exchange of a particle during the volatile yield is described:

$$m_p c_p \frac{\mathrm{d}T_p}{\mathrm{d}t} = \alpha S_p \left(T_\infty - T_p\right) + \frac{\mathrm{d}m_p}{\mathrm{d}t} h_v \tag{22}$$

$$\frac{\mathrm{d}m_p}{\mathrm{d}t} = -f_{v,0} m_{p,0} k \tag{23}$$

The kinetic reaction rate is determined by the Arrhenius equation:

$$k = A_1 \mathrm{e}^{-\left(E/\mathrm{R}T_p\right)} \tag{24}$$

This volatile yield model suggests that the rate of volatile yield primarily depends on the amount of volatiles remaining in the particle [29].

The coke residue burnout model is applied at the end of the volatile release until the entire coke residue burns out: $(1 - f_{v,0} - f_k)m_{p,0} \leq m_p \leq (1 - f_{v,0})m_{p,0}$.

This model of coke burnout suggests that the surface reaction rate is determined by both kinetic and diffusion components. The heat and mass exchange of a particle during coke residue burnout is described:

$$m_p c_p \frac{\mathrm{d}T_p}{\mathrm{d}t} = \alpha S_p \left(T_\infty - T_p\right) - f_h \frac{\mathrm{d}m_p}{\mathrm{d}t} H_u \tag{25}$$

$$\frac{\mathrm{d}m_p}{\mathrm{d}t} = -S_p P_{O_2} \frac{D_0 R}{D_0 + R} \tag{26}$$

The coefficient of diffusion reaction rate is determined:

$$D_0 = C_1 \frac{\left(\frac{T_p + T_\infty}{2}\right)^{0.75}}{d_p} \tag{27}$$

The kinetic rate coefficient of the reaction is determined:

$$R = C_2 \mathrm{e}^{-\left(E/\mathrm{R}T_p\right)} \tag{28}$$

After the entire coke residue burns out, the particle consists of an ash residue, and the model of heat exchange of an inert particle is valid for it, eq. (21). Discretization of the initial PDE (1)-(7) is carried out by means of the control volume method using a first-order accuracy scheme for approximating convective terms. The control volume method is also used in [1-10, 14-16, 21-24]. The solution of the resulting systems of linear algebraic equations is solved by the Gauss-Seidel method using the SIMPLE algorithm [33]. Integro-differential eq. (8) is solved by the method of spherical harmonics [30, 31, 33]. The system of ODE (21)-(27) is integrated using the Runge-Kutta method. To calculate the conditions of chemical equilibrium, an algorithm based on minimizing the Gibbs free energy is used.

The solution is found in the calculation area corresponding to the flow part of the furnace. The computational domain is covered by an uneven polygonal grid, which includes 64.265 control cells.

The boundary conditions of the continuous phase are set at the boundaries of the computational domain: at the incoming sections – the value of independent variables; on the walls – adhesion conditions; in the initial region – *soft* boundary conditions. Empirical wall functions are used to describe the turbulent boundary layer [32]. When modeling the discrete phase, the initial conditions are set for each calculated particle: the particle position (x_j coordinates), its velocity (u_{ps} components), diameter, temperature, as well as the mass-flow rate of particles following along the trajectory. It is taken into account that when they collide with the walls, the particles elastically repel them. The creation of a furnace with oncoming swirling flows is based upon the researches in [34].

Figure 1 shows a general view (sections, isometry) of the furnace and the main geometric dimensions are indicated.

Figure 2 shows the design grids of the furnace, inlet and outlet channels.

On the boundaries of the computational domain the following boundary conditions of the external phase are set: on the inlet sections – the value of the independent variables; on the walls – no-slip conditions; on the initial section - “soft” boundary conditions. To describe the turbulent boundary layer empiric wall functions are used.

While modeling the discrete phase, the initial conditions for each calculated particle are set: the position of the particle, its velocity, diameter, temperature, and the mass-flow of particles along the trajectory. It is taken into account that colliding with the walls the particles are elastically pushed off them.

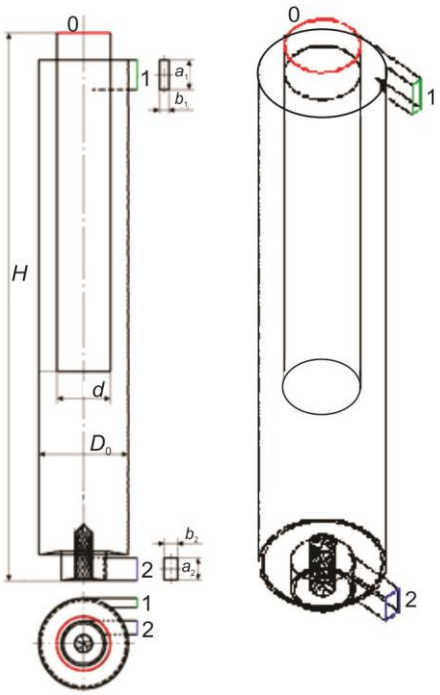

Figure 1. Design of the furnace with the countercurrent swirl flows: 1 – inlet of the air mixture, 2 – inlet of secondary air, and 0 – outlet of flue gases; dimensions of swirler sections: a_1 = 0.198 m, b_1 = 0.06 m, a_2 = 0.15 m, b_2 = 0.-05 m

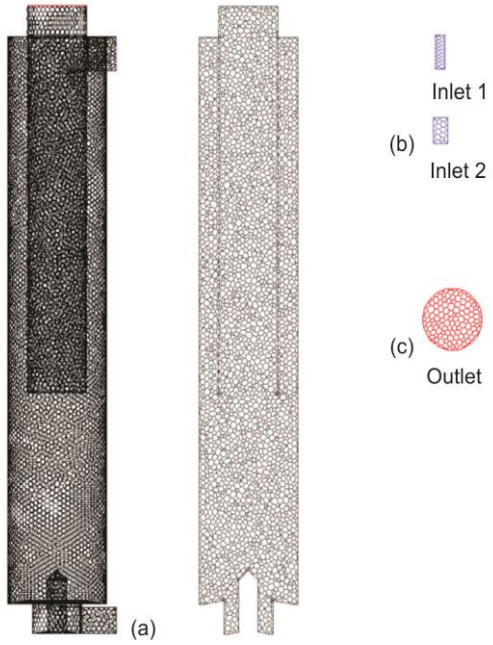

Figure 2. Design grids of the furnace, input and output channels [35, 36]: (a) furnace: surfaces, sections, (b) swirler outlet sections, and (c) the outlet section of the exhaust pipe

Results and discussions

The following parameters are adopted in this paper: the external diameter of the furnace is 600 mm, the height of the furnace is 3465 mm. The heat power of the furnace is 2.5 MW. The total air excess ratio is α_a = 1.9. The furnace is made as a heat-insulated (adiabatic) one. The calculation results of the furnace being cooled indicate the uncompleted combustion of solid peat particles. The chemical peat composition (for combustible mass) is the following: C – 56%, H – 6%, O – 35%, N – 2%, and S – 1%. The technical peat composition (for working mass) is the following: volatile – 38%, coke – 16%, ash content – 6%, and humidity – 40%. The stoichiometric peat coefficient is V_0 = 3.7. The temperature of the beginning of the peat devolatilization is 100 °C. The highest peat combustion heat value (for working mass) is Q = 12.3 MJ/kg. The composition of the slag and the melting point of the slag are taken according to [7].

The dispersed composition of peat dust is presented in figs. 3 and 4 with a histogram of the distribution of mass fractions of peat particles by their size and grain characteristics. Dust is characterized by the following sieve residues: R90 = 17%, R200 = 2.5% and is fine dust.

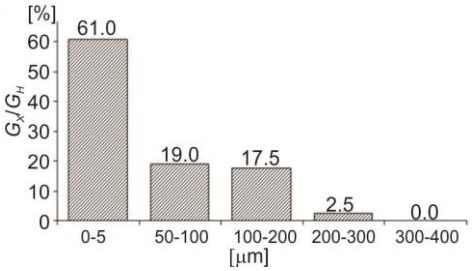

Figure 3. Distribution of mass fractions of peat particles by their size

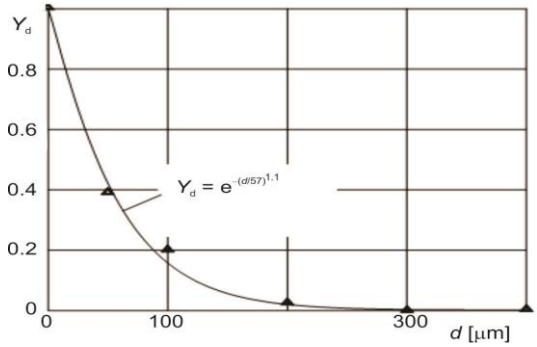

Figure 4. Integral granular peat dust characteristics

The main results of the calculations are shown in table 1.

Table 1. Calculation results

Parameter, [unit]	Furnace version number				
	1	2	3	4	5
D_a [mm]	600	1100	600	600	600
H [mm]	3645	6683	3645	3645	3645
m_f [kgs^{-1}]	0.18	0.6	0.09	0.027	0.18
W [MW]	2.5	7.5	1.25	0.375	2.5
$\overline{W}$ [%]	100	100	50	15	100
m_{a1} [kgs^{-1}]	1.26	4.2	0.63	0.189	1.26
t_{a1} [°C]	377	377	377	377	377
m_{a2} [kgs^{-1}]	0.315	1.05	0.1575	0.04725	0.315
$m_{a\Sigma}$ [kgs^{-1}]	1.575	5.25	0.7875	0.23625	1.575
a_1^*	1.9	1.9	1.9	1.9	1.9
a_Σ^*	2.36	2.36	2.36	2.36	2.36
$d_{h.\min}$ [μm]	25	25	25	25	25
$d_{h.\min}$ [μm]	250	250	250	250	250
$\overline{d}$ [μm]	57	57	57	57	57
$t_{g.\text{out}}$ [°C]	1711	1719	1684	1559	704
$t_{\text{cinder,out}}$ [°C]	1380	1000	1330	1280	420
$g_{O2.\text{out}}$ [%]	5.2	5.2	5.2	5.2	7
The degree of volatile burnout, [%]	100	100	100	100	100
The degree of coke burnout, %	99.8	100	100	100	61.8
Mechanical underburning (of combustible mass), [%]	0.06	0	0	0	21.1
Particle trapping, [%]	47.6	47.4	44.3	19.9	90.6
Particle removal, [%]	52.4	52.6	55.7	80.1	9.4

*were $\alpha_1 = m_{a1} / m_f V_0$; $\alpha_\Sigma = m_{a\Sigma} / m_f V_0$

Analysis of the calculation results given in table 1 shows the following:

– the temperature of the flue gases reaches a value of 1952 °C, while the minimum proportion of oxygen is 0.5% and

– when mixed with secondary air, the temperature in the furnace volume decreases to (1300-1450 °C) and an increase in the mass fraction of oxygen to 5.2% is observed at the outlet of the furnace.

The temperature of ash removed along the wall of the furnace is 1380 °C. Moisture evaporation, the yield of volatiles and their combustion lead to the fact that the maximum absolute gas velocity reaches 372 m/s in the upper part of the furnace, and decreases to values of 150-170 m/s in the middle zone of the furnace, in the torch zone. Secondary air is supplied at high speed, which ensures the uniform filling of the torch in the furnace volume and, therefore, the time of coke part staying in the furnace increases.

The analysis of particle motion trajectory, figs. 6-10, shows that particles with a diameter of 25 μm enter the upward flow of flue gases and are carried away from the furnace, while particles with a diameter of 250 μm settle in the lower part of the furnace. Volatiles burn out from particles with diameters of 25 μm and 250 μm. Coke (non-volatile powder residue - carbon and mineral part) burns out from particles with a diameter of 25 μm. Depending on the particle diameter, coke burns out in different ways.

The trajectory of particles in the furnace is affected by the moisture and volatile yield from the fuel particles. Moisture is removed at the furnace inlet in the upper part, the concentration of small particles is high in the lower zone of the furnace, and large particles are concentrated in the upper zone of the furnace. Volatiles are released from small particles (25 μm) at the furnace inlet and their concentration increases in the lower zone of the furnace, and large particles are concentrated in the upper zone of the furnace since the volatile yield from them is slower.

Thus, moisture is released from the particles at the furnace inlet in the upper zone and is removed with the flue gases. The ash of small particles is removed from the furnace along with flue gases, and the ash of large particles is captured and removed to the hopper in the lower zone of the furnace (44.3-47.6%). Volatiles burn completely (100%), and solid particles have a mechanical underburning (up to 0.06%) and ash removal of 52%. Coke from particles with an initial diameter of up to 200 μm burns out completely; coke from particles with an initial diameter of 250 μm in the composition of fine dust from 25 μm to 250 μm burns out by 96%; coke from particles with initial diameters of 100 μm, 325 μm, and 550 μm in the composition of coarse dust from 100 μm to 1000 μm burns out by 79%, 35%, and 5%, respectively; coke from particles with initial diameters greater than 775 μm in the composition of coarse dust from 100 μm to 1000 μm practically does not burn out; scaling the furnace by increasing its geometric dimensions by 1.83 times and the rated heat capacity by three times (option No. 2) leads to a decrease in the final ash temperature to 1000 °C and a decrease in mechanical underburning; decrease in heat load up to 50% and up to 15% (option No. 3 and No. 4) results in:

– lowering the gas temperature at the outlet by 1.6% and 9%, respectively,
– lowering the final temperature of ash to 1330°C and 1280°C, respectively, and
– lowering the ash removal up to 56% and up to 80%, respectively.

Cooling the furnace body (option No. 5) (t = 120 °C) leads to a decrease in the temperature of gases up to 704 °C, the degree of burning of coke from particles that are carried away is 61.8% and from particles that are trapped is 28.6%. Analysis of coke burning depending on the particle diameter (adiabatic furnace) is the following: the results of the numerical study are presented in figs. 5-10. The gas temperature distribution fields in the furnace volume are presented in fig. 5(a). High temperature combustion of peat takes place in the furnace. As it can be seen the gases temperature increases along the furnace height and reaches a

value of 1711 °C at the outlet from the furnace. After that the gases purified from solid particles enter the furnace which is shielded by tube bundles and they are cooled.

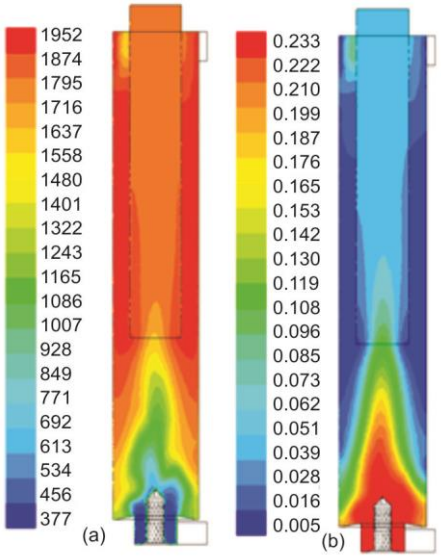

Figure 5. Distribution of gas phase parameters in the longitudinal section of the furnace with the countercurrent swirl flow: (a) gas temperature, (b) oxygen mass fraction

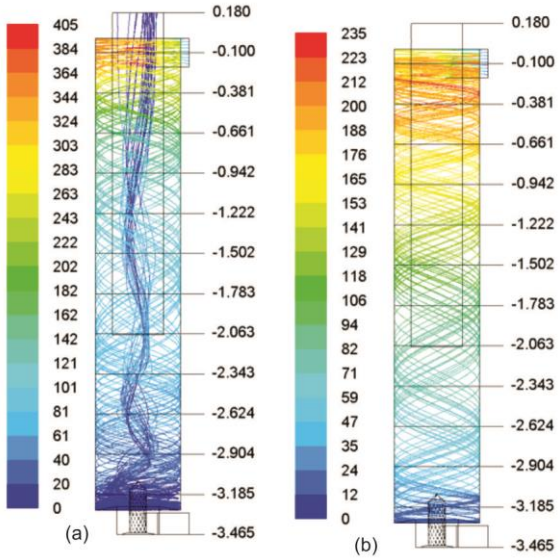

Figure 6. Trajectories of peat particles with initial diameters of 25 μm (a) and 250 μm (b), colored according to the tangential component of their velocity [ms^{-1}]

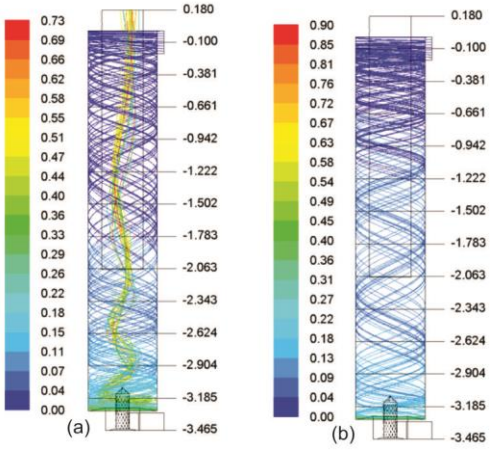

Figure 7. Trajectories of peat particles with initial diameters of 25 μm (a) and 250 μm (b), colored according to their time of coke part staying in the furnace

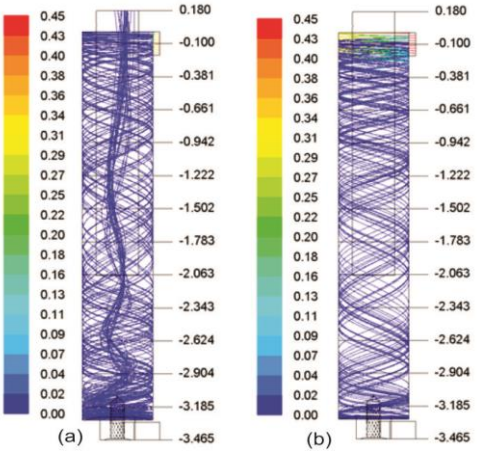

Figure 8. Trajectories of peat particles with initial diameters of 25 μm (a) and 250 μm (b), colored according to the mass moisture fraction in their composition

The completeness of solid fuel particle combustion is confirmed by the oxygen distribution fields along the furnace height, fig. 5(b). From any furnace height the oxygen concentration is close to zero, at the outlet from the furnace the oxygen concentration is 5% and 6%, as the oxygen is supplied with excess (α_a = 1.9). Mechanical underburning is 0.06%.

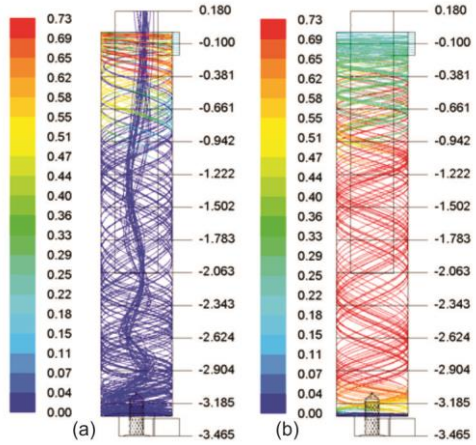

Figure 9. Trajectories of peat particles with initial diameters of 25 μm (a) and 250 μm (b), colored according to the mass fraction of coke in their composition

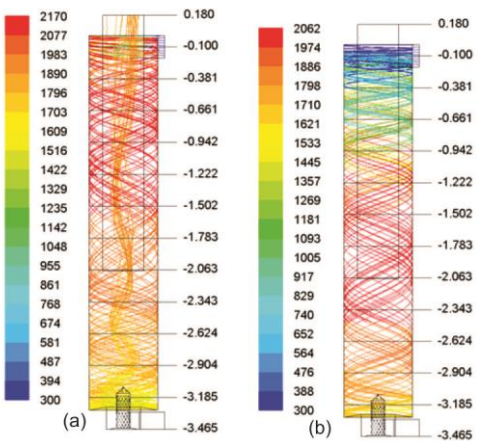

Figure 10. Trajectories of peat particles with initial diameters of 25 μm (a) and 250 μm (b), colored according to their temperature [°C]

The effect of the particle size can be noted. The coarse grains are in the furnace up to the complete combustion.

Volatiles manage to escape from any particles (from 25 to 250 μm) within the upper part of the annular section of the furnace, but coke has time to burn out only from the smallest particles within the annular section of the furnace (25 μm). The degree of the coke burnout is 97.7%. There is a significant removal of fine particles. The flue gas temperature is 1478 °C.

Conclusions

As a result of numerical study of simulating peat dust particle combustion processes, the influence of the design factors of the furnace (diameter, height), the expenditure of primary and secondary air and their ratios, the fuel supply method (from the bottom of the furnace, from the top one) is determined. The advantages of a top fuel supply have been found. The processes of peat combustion in cooled and thermally insulated (lined) furnaces have been studied. The combustion of peat particles is found to take place at lower temperatures (1300-1450 °C). At the same time, conditions are provided to reduce NO_x emissions. The particles of a small diameter (about 25 microns) are not in the furnace for long but enough for their combustion. Peat combustion at a high temperature in furnace volume occurs when forming liquid slag which is removed through an opening at the bottom of the furnace. The results of a numerical study show that the diameter of peat particles affects the process of their combustion: coke particles with initial diameters from 25 μm to 250 μm burn out by 96%. Increasing a particle diameter up to 1000 μm, the degree of coke burnout decreases but at the same time their removal decreases. In general, while modeling the technology of low-calorie dusty solid fuel combustion in cylindrical vortex furnace with countercurrent swirl flows has effectively been used.

Nomenclature

A_1 – preexponential factor [molS^{-1}]
C_1 – empirical coefficient [–]
C_2 – preexponential factor [molS^{-1}]
C_μ – empirical coefficient [–]
c_{pi} – specific heat capacity of chemical component i at constant pressure [kJmol^{-1}K^{-1}]
C_R – aerodynamic drag coefficient of a particle [–]

c_p – specific heat capacity of the particle [kJkg^{-1}K^{-1}]
D_0 – diffusion velocity coefficient [–]
d_p – particle diameter [m]
$\bar{d}$ – median particle diameter [m]
E – activation energy [Jmol^{-1}]
f_k – mass fraction of coke originally present in the particle [–]
f_h – empirical coefficient [–]
$f_{v,0}$ – mass fraction of volatiles initially present in the particle [–]
G – term characterizing the generation of kinetic energy of turbulence due to shear stresses [–]
h – instantaneous enthalpy [Jmol^{-1}]
H_u – specific heat of coke combustion [Jmol^{-1}]
h_v – specific heat of formation of volatile particles [Jmol^{-1}]
Δh_{fi}^0 – specific enthalpy of formation of chemical component i [Jmol^{-1}]
I_b – radiation intensity of a completely black body (= $\sigma T^4/\pi$) [Wm^2]
I – radiation intensity [Wm^3]
k – kinetic reaction rate [moleS^{-1}]
k_a – volumetric absorption coefficient [–]
m_{a1} – mass-flow rate of primary air [kgs^{-1}]
M_i – molecular weight of the chemical component i [gmol^{-1}]
m_p – particle mass [kg]
m_{a2} – mass-flow rate of secondary air [kgs^{-1}]
$m_{a\Sigma}$ – mass air-flow rate [kgs^{-1}]
m_f – mass fuel consumption [kgs^{-1}]
$m_{p,0}$ – initial particle mass [kg]
n – distribution parameter [–]
P – gas pressure [Pa]
p_{O2} – partial pressure of oxygen in the gas [Pa]
$P_n(f_n)$ – PRV function describing the probability that the value of the variable φ_i is between φ and $\varphi + \Delta\varphi$ and approximated by β function [–]
Pr – Prandtl number [–]
Pr_T – turbulent Prandtl number [–]
Re_p – relative Reynolds number of a particle [–]
R – kinetic reaction rate coefficient [m^{2}mole^{-1}S^{-1}]
$\vec{r}$ – radius-vector of an arbitrary ray in the angular direction of radiation propagation $\vec{S}$ [m]
S_p – particle surface area [m^2]
S_q – heat source due to interfacial interaction with particles [J]
S_{fj} – source of momentum due to interphase interaction [–]
S_n – mass source corresponding to the mass transfer to the gas phase from reacting particles [mol]
T – gas temperature [K]
T^0 – standard temperature [K]
t – time [s]
T_p – particle temperature [K]
T_∞ – local gas temperature [K]
$t_{\mathrm{g,\ out}}$ – temperature of the flue gases at the outlet of the furnace [°C]
$t_{\mathrm{з,\ out}}$ – ash temperature at the outlet [°C]
t_{a1} – primary air temperature [°C]
u_{pj} – cartesian components of the particle velocity vector [ms^{-1}]
u_j – cartesian components of the averaged gas velocity vector [ms^{-1}]
u_i' – gas velocity perturbations relative to the averaged value [ms^{-1}]
W – thermal power of the furnace, [MW]
$\overline{W}$ – thermal power [%]
x_j – cartesian coordinates [m]
Y_i – mass fraction of the chemical component i [–]
Y_d – mass fraction of particles with a diameter greater than d [–]

Greek symbols

α_1 – mass fraction of primary air, [–]
α_Σ – coefficient of excess air [–]
α – heat transfer coefficient [Wm^{-2}K^{-1}]
β_0 – volumetric attenuation coefficient (= $k_a + \sigma_s$) [–]
ε – specific rate of dissipation of turbulent kinetic energy [m^{2}s^{-3}]
λ – coefficient of thermal conductivity [WK^{-1}]
μ – dynamic viscosity [Pa·s]
μ_T – is turbulent viscosity [Pa·s]
ν – coefficient of kinematic viscosity [m^{2}s^{-1}]
Ω' – unit solid angle vector characterizing the direction of propagation of thermal radiation due to photon scattering $\vec{S}'$ [steradian]
ρ – density [kgm^{-3}]
ρ_p – particle density [kgm^{-3}]
σ_s – volume scattering coefficient [m^{-1}]
$\sigma_k, \sigma_\varepsilon, C_{\varepsilon 1}, C_{\varepsilon 2}$ – empirical coefficients [–]
σ – Stefan-Boltzmann constant [Wm^{-2}K^{-4}]
σ_s – volumetric scattering coefficient [m^{-1}]
$\sigma_\mathrm{T}, C_g, C_d$ – are empirical coefficients [–]
τ_{ij} – components of the stress tensor [Pa]
ω_0 – scattering albedo (= σ_s/β_0)[–]

References

[1] Basu, P., Biomass Gasification and Pyrolysis. Practical Design and Theory, Elsevier, Amsterdam, The Netherlabd, 2010
[2] Serant, F. A., *et al*. *Burning Asian Old Brown Coals in a Low Temperature Vortex Furnace According to the Scheme LPI-ITES-10* (in Russian), Thermal Engineering, 1983
[3] Rundygin, Yu. A., *et al*., Modernization of Boilers Based on Low Temperature Vortex Technology for Burning Solid Fuels, *Energy: Economics, Technology, Ecology*, *4* (2000), pp. 19-22
[4] Shestakov, S. M., *et al*., *Technology of Combustion of Local Solid Fuel Types*, Saint Petersburg State Polytechnic University, Saint Petersburg, Russia, 2014
[5] Baskakov, A. P., *et al*., *Boilers and Furnaces with a Fluidized Bed*, Energoatomizdat, Moscow, Russia, 1996
[6] Shtym, A. N., *et al*., *Kotelnye Ustanovki s Tsyclonnymi Predtopkami* (Boiler Installations with Cyclone Prefabs – in Russian), Dom Dalnevostochnyi Federalnyi Universitet, Vladivostok, Russia, 2012
[7] Dolejal, R. N., *Furnaces with Liquid Slag Removal* (in Russian), GosEnergoizdat, Moscow, Russia, 1959
[8] Khzmalyan, D. M., *Theory of Furnace Processes* (in Russian), Energoizdat, Moscow, Russia, 1990
[9] Knorre, G. F., *et al*., *Cyclone Furnaces* (in Russian), GosEnergoizdat, Moscow, Russia, 1959
[10] Marshak, Yu. L., *Furnaces with Vertical Cyclone Prefurnaces* (in Russian), Energy, 1966
[11] Philip, J., Stopford Recent Application of CFD Modelling in the Power Generation and Combustion Industries, *Applied Mathematical Modelling*, *26* (2002), 2, pp. 351-374
[12] Al-Abbas, A. H., *et al*., Computational Fluid Dynamic Modelling of a 550 MW Tangentially – Fired Furnance Under Different Operation Conditions, *Procedia Engineering*, *56* (2013), May, pp. 387-392
[13] Lv, T., *et al*., Numerical and Experiment Research for Soft Coal under Condition of Blending Lignite, *Energy Procedia*, *17* (2012), B, pp. 1001-1006
[14] Safarik, P., *et al*., 3-D Modelling of Heat and Mass Transfer during Combustion of Low-Grade Coal, *Thermal Science*, *24* (2020), 5A, pp. 2823-2832
[15] Safarik, P., *et al*., 3D Modeling the Activated Combustion Thermochemical Fuel, *News of the National Academy of Sciences of the R. of Kazakhstan-Series Physico-Mathematical*, *2* (2019), 324, pp. 9-16
[16] Anikin, Yu. A., *et al*. Vortex Steam Generator of a New Type Modeling of Furnace Processes, *Proceedings*, VIII All-Russian Conference with the International Part "Combustion of Solid Fuel" Institute of Thermophysics named after S.S. Kutateladze SORAN, Novosibirsk, Russia, 2012, pp. 51-66
[17] Glushkov, D. O., *et al*., Numerical Research of Heat and Mass Transfer During Low Temperature Ignition of a Coal Particle, *Thermal Science*, *19* (2015), 1, pp. 285-294
[18] Chen, X., *et al*., Thermal Analyses of the Lignite Combustion in Oxygen-Enriched Atmosphere, *Thermal Science*, *19* (2015), 3, pp. 801-811
[19] Lomovsky, O., *et al*., Mechanochemical Production of Lignin-Containing Powder Fuels from Biotechnical Industry Waste: A Review, *Thermal Science*, *19* (2015), 1, pp. 219-229
[20] Redko, A., *et al*., Low Temperature Energy Systems with Applications of Renewable Energy, Elsevier Academic Press, New York, USA, 2019
[21] LaRose, J. A., *et al*., Numerical Flow Modeling of Power Plant Windboxes, *Proceedings*, Power-Gen Americas 95, Anaheim, Cal., USA, 1995
[22] Bhasker, C., Simulation of Air-Flow in the Typical Windbox Segments, *Adv. Eng. Software*, *33* (2002), 11-12, pp. 793-804
[23] Filkoski, R., *et al*., Optimisation of Pulverised Coal Combustion by Means of CFD/CTA Modelling, *Thermal Science*, *10* (2006), 3, pp. 161-179
[24] James, T., *et al*., Numerical Modelling of Unsteady Flow Behaviour in the Rectangular Jets with Oblique Opening, *Alexandria Engineering Journal*, *55* (2016), 3, pp. 2309-2320
[25] Buthalura, R., *et al*., Modelling, of a Wall-Fired Furnace for Different Operating Conditions Using Fluent, *Fuel Process. Technol.*, *87* (2006), 7, pp. 633-639
[26] Crow, D., *Numerical Models of Gas Flows with a Small Content of Particles* (in Russian), Foundations of Engineering Calculations, 1982
[27] Launder, B. E., *et al*., *Lectures in Mathematical Models of Turbulence*, Academic Press, London, 1972, p. 169
[28] Jones, W. P., Whitelaw, J. H., Calculation Methods for Reacting Turbulent Flows: A Review, *Combustion and Flame*, *48* (1982), Aug., pp. 1-26
[29] Loitsyanskii, L. G., *Mechanics of Fluid and Gas* (in Russian), Nauka, Moscow, Russia, 1978

[30] Chui, E. H., *et al*., Computation of Radiant Heat Transfer on a Noh – Orthogonal Mesh Using the Finite – Volume Method, *Numerical Heat Transfer. Part B: Fundamentals*, *23* (1993), 3, pp. 269-288
[31] Bass, L. P., *et al*., *Methods of Discrete Ordinate in Radiation Transfer Problems*, Institute of Applied Mathematics, USSR Academy of Sciences, Moscow, 1986
[32] Badzioch, S., *et al*., Kinetics of Thermal Decomposition of Pulverized Coal Particles, *Ind. Eng. Chem. Process Design and Development*, *9* (1970), 4, pp. 521-530
[33] Surzhikov, S. T., *Thermal Radiation of Gases and Plasma* (in Russian), Bauman Moscow State Technical University, Moscow, Russia, 2004, p. 544
[34] Sazhyn, B. S., *et al*., *Vortex Dust Collectors* (in Russian), Federal State Budgetary Educational Institution of Higher Education A.N. Kosygin, Moscow, Russia, 1995
[35] ***, Engineering Simulation & 3-D Desing Software [ANSYS], https://www.ansys.com/
[36] Poinsot, T., *et al*., *Theoretical and Numerical Combustion*, 2nd ed., R. T. Edwards. Inc., 2005, p. 522

Paper submitted: March 5, 2019
Paper revised: March 16, 2020
Paper accepted: April 7, 2020